HHS Public Access

Author manuscript

*Mol Pharm*. Author manuscript; available in PMC 2016 July 27.

Published in final edited form as:

*Mol Pharm*. 2015 June 1; 12(6): 2010–2018. doi:10.1021/mp5008212.

# CD33-Targeted Lipid Nanoparticles (aCD33LNs) for Therapeutic Delivery of GTI-2040 to Acute Myelogenous Leukemia

**Hong Li**[†], **Songlin Xu**[†], **Jishan Quan**[†,⊥], **Bryant C. Yung**[†], **Jiuxia Pang**[‡], **Chenguang Zhou**[†], **Young-Ah Cho**[†], **Mengzi Zhang**[§], **Shujun Liu**[‡], **Natarajan Muthusamy**[‡], **Kenneth K. Chan**[†], **John C. Byrd**[‡], **L. James Lee**[‖], **Guido Marcucci**[‡], and **Robert J. Lee**[*,†]

[†]Division of Pharmaceutics, College of Pharmacy, The Ohio State University, Columbus, Ohio 43210, United States

[‡]Division of Hematology-Oncology, The Ohio State University, Columbus, Ohio 43210, United States

[§]Molecular, Cellular and Developmental Biology Program, The Ohio State University, Columbus, Ohio 43210, United States

[‖]Department of Chemical and Biomolecular Engineering, The Ohio State University, Columbus, Ohio 43210, United States

[⊥]Pharmacy College, Yanbian University, Yanji, Jilin 133002, China

## Abstract

CD33-targeted lipid nanoparticles (aCD33LNs) were synthesized for delivery of GTI-2040, an antisense oligonucleotide (ASO) against the R2 subunit of ribonucleotide reductase, to acute myelogenous leukemia (AML). These LNs incorporated a deoxycholate-polyethylenimine (DOC-PEI) conjugate, which has shown significant activity to facilitate oligonucleotide delivery. Anti-CD33 scFv (aCD33) was added as a targeting ligand. The delivery efficiency of this system was investigated both *in vitro* and *in vivo*. When cells were treated with aCD33LN/GTI-2040, significant uptake was observed in CD33 positive Kasumi-1 cells. aCD33LNs loaded with GTI-2040 induced significant downregulation of R2 mRNA and protein levels in AML cells. Moreover, aCD33LN/GTI-2040 showed a 15-fold reduction in the $IC_{50}$ of antileukemic drug Ara-C in Kasumi-1 cells. In Kasumi-1 xenograft model, aCD33LN/GTI-2040 showed significant R2 downregulation compared to LN/GTI-2040. Furthermore, aCD33LN/GTI-2040 coadministered with Ara-C was shown to be highly effective in tumor growth inhibition and to greatly increase survival time of mice bearing Kasumi-1 xenograft tumors. The conjugate DOC-PEI has shown an ability to include calcein release from lipid nanoparticles, suggesting a potential mechanism contributing to efficient endosome release by DOC-PEI2K. These results indicate that aCD33LNs are a highly effective vehicle for the therapeutic delivery of antisense agents to AML.

## Graphical abstract

[*]**Corresponding Author** Address: College of Pharmacy, 500 West 12th Avenue, Columbus, Ohio 43210, Unites States. Phone: (614) 292-4172. lee.1339@osu.edu.

Notes

The authors declare no competing financial interest.

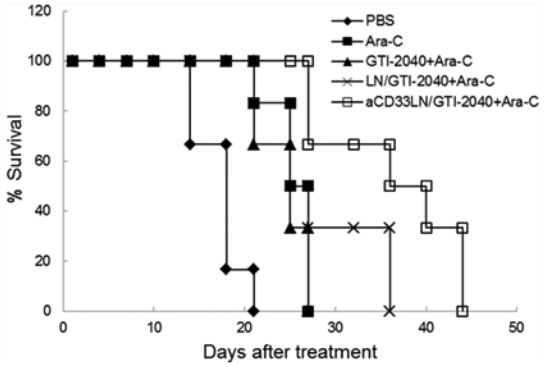


**Keywords**

CD33-targeting; lipid nanoparticles; deoxycholate-polyethylenimine conjugate; acute myelogenous leukemia; antisense oligonucleotide; GTI-2040

## 1. INTRODUCTION

Antisense oligonucleotide (ASO) therapy is an emerging modality for the treatment of human diseases.[1–3] Recently, mipomersen, an ASO against apolipoprotein-B, has been approved by the FDA for familial hypercholesterolemia.[4] However, ASOs have been less successful as therapeutic agents against cancer and leukemia. This can partially be attributed to the rapid clearance of the ASOs, their low membrane permeability, and the lack of an effective delivery system.[5,6] Lipid nanoparticles (LNs) have shown promise as delivery vehicles for ASOs.[7–9] However, further improvement in their effciency is important for their successful application in the clinic. This can be accomplished by further optimization of their composition and by introducing a targeting moiety to facilitate selective delivery to the targeted cell population.

Acute myelogenous leukemia (AML) is a common leukemia in adults and currently has poor clinical outcome.[10,11] An attractive therapeutic target is the ribonucleotide reductase (RNR), which is required for intracellular conversion of NTP to dNTP. Cytarabine (Ara-C) is frequently used for the treatment of AML. RNR overexpression is a major mechanism for chemoresistance of AML to Ara-C. Therefore, down regulation or inhibition of RNR by ASO can inhibit leukemia cell proliferation and sensitize it to chemotherapeutic agents such as Ara-C. GTI-2040, also known as LOR-2040, is a 20-mer phosphorothioate antisense oligonucleotide targeting the mRNA of R2 subunit of RNR (RNR R2 or RRM2).[12] It has been evaluated in a Phase I clinical trial in AML in combination with Ara-C, which showed that treatment with GTI-2040 was safe and some evidence of reduction of R2 target in patients.[13] Therefore, further improvements in the efficacy of GTI-2040 are likely needed to facilitate further development of this agent.

In this study, a novel lipid nanoparticle formulation was synthesized and evaluated for the delivery of GTI-2040 into AML cells. A cationic agent, deoxycholate-polyethylenimine conjugate (DOC-PEI), was synthesized and incorporated into the LNs to facilitate endosomal release of the ASO. In addition, a single-chain variable fragment (scFv) against

CD33, a surface marker for myeloid cells,[14] was incorporated in the LNs via a hydrophobic anchor to facilitate selective delivery to AML cells.[15–18] The pharmacological activity of aCD33LN/GTI-2040 was evaluated both in AML cells and in xenograft tumors derived from AML cells. Its therapeutic activity was assessed alone and in combination with Ara-C.

## 2. MATERIALS AND METHODS

### 2.1. Materials

2,3-Dioleyloxy-propyl-trimethylammonium chloride (DOTAP) and dioleoylphosphatidylethanolamine (DOPE) were purchased from Genzyme Corporation (Cambridge, MA, USA). D-*α*-Tocopheryl polyethylene glycol-1000 succinate (TPGS) was purchased from Eastman Co. (Kingsport, TN, USA). Egg phosphatidylcholine was purchased from Avanti Polar Lipids (Alabaster, AL, USA). Cholesterol, DOC, PEI (MW 2000), *cis*-11-hexadecenal, glycine, and bovine serum albumin (BSA) were purchased from Sigma-Aldrich Chemical Co. (St. Louis, MO, USA). 1-Ethyl-3-[3-(dimethylamino)propyl] carbodiimide hydrochloride (EDC) and *N*-hydroxysulfosuccinimide (Sulfo-NHS) were purchased from Thermo Scientific (Rockford, IL, USA). GTI-2040 (5′-GGCTAAATCGCTCCACCAAG-3′), GTI-2040 scrambled control oligodeoxynucleotide (sGTI-2040) (5′-ACGCACTCAGCTAGTGACAC-3′), and Cy5-labeled GTI-2040 were custom synthesized by Alpha DNA (Montreal, Quebec, Canada). TRIzol Reagent and Hoechst 33342 were purchased from Life Technologies (Carlsbad, CA, USA). The anti-CD33 scFv, aCD33, was a generous gift from Dr. Peter J. Nicholls at the Department of Biosciences, University of Kent, U.K.

### 2.2. Cell Culture

Kasumi-1 (a human AML cell line) and K562 (a human chronic myelogenous leukemia cell line) cells were obtained from ATCC (Manassas, VA, USA). Kasumi-1 cells were maintained in RPMI 1640 (Gibco, CA, USA) media supplemented with 20% heat-inactivated fetal bovine serum (FBS) (Gibco, CA, USA), penicillin, and streptomycin. K562 cells were cultured in RPMI 1640 media supplemented with 10% heat-inactivated FBS, penicillin, and streptomycin. All cells were grown in a humidified atmosphere containing 5% $CO_2$ at 37 °C.

### 2.3. Synthesis of DOC-PEI

DOC-PEI conjugate was synthesized by forming an amide bond between the DOC and PEI (MW 2000). Briefly, 400 mg of DOC and 200 mg of PEI were dissolved in 4 mL of dd$H_2O$ with pH adjusted to 8.0. The reaction was initiated by addition of 50 mg of sulfo-NHS and then 200 mg of EDC. The reaction mixture was incubated at room temperature for 2 h. Then, the product was purified by dialysis against dd$H_2O$ water using a Slide-A-Lyzer (Pierce, Rockford, IL, USA) dialysis membrane (MWCO, 2 kDa) overnight at room temperature with periodic replacement of the external water. Finally, the product was lyophilized for 48 h and stored at −20 °C until use. The structure of DOC-PEI was characterized by Fourier transform infrared (FT-IR) spectroscopy and proton nuclear magnetic resonance ($^1$H NMR) spectroscopy analyses.

### 2.4. Synthesis and Characterization of GTI-2040 Loaded LNs (LN/GTI-2040)

First, cationic liposomes were prepared by an ethanol dilution method. Briefly, lipids with the composition of DOTAP/DOPE/cholesterol/TPGS (40:10:45:4 mol/mol), with or without the additional 1 mol % *cis*-11-hexadecenal (used for synthesis of aCD33 conjugated LNs), were dissolved in ethanol and injected into HEPES buffer (10 mM, plus 5% glucose, pH 7.4) to spontaneously form cationic liposomes. The liposomes were dialyzed against HEPES buffer for 2 h at room temperature using a Slide-A-Lyzer dialysis membrane (MWCO, 10 kDa) and then collected in a vial and stored at 4 °C.

LN/GTI-2040 was prepared by adding DOC-PEI dissolved in HEPES buffer into the liposomes prepared above (without *cis*-11-hexadecenal), followed by GTI-2040, which was also dissolved in HEPES buffer. The molar ratio of total lipids/DOC-PEI/ODN used was 10:1:1 (w/w). The LNs were allowed to form by self-assembly.

For preparation of CD33 targeted LN/GTI-2040, aCD33 (scFv) was incubated with cationic liposomes containing 1 mol % *cis*-11-hexadecenal at 37 °C for 1 h at a protein to lipid molar ratio of 1:100 to enable conjugation of aCD33 to the surface of liposomes. This is followed by addition of DOC-PEI and GTI-2040. aCD33 was conjugated to the surface of the LNs by forming a Schiff base (–C=N–) linkage between the carbonyl of *cis*-11-hexadecenal and a primary amine from aCD33.[19]

The particle size and zeta potential of LN/GTI-2040 and aCD33LN/GTI-2040 were measured on a Nicomp model 370 Submicron Particle Sizer (Particle Sizing Systems, CA, USA) and Zeta PALS (Brookhaven Instruments Co., NY, USA), respectively.

### 2.5. Effect of DOC-PEI in LNs on Transfection Efficiency *in Vitro*

Kasumi-1 cells were seeded in a 6-well plate at a density of $5 \times 10^5$ cells/mL and cultured for 18 h prior to transfection. During transfection, culture media was replaced with LN/GTI-2040 containing DOC-PEI or LN/GTI-2040 containing PEI-2K (at the same PEI level) in serum-free media for 4 h. Then, the cells were incubated at 37 °C for an additional 48 h. R2 protein was extracted from the cell lysate and evaluated by Western blot. GAPDH was selected as a housekeeping gene to which R2 was normalized.

### 2.6. Membrane Lytic Activity of DOC-PEI on Liposomes

Liposomes encapsulating calcein were prepared by thin film hydration followed by polycarbonate membrane extrusion, as described previously.[20] The lipids used in the liposomes were egg PC and cholesterol at a molar ratio of 7:3. DOC-PEI or PEI-2K with the same PEI content was added to calcein liposomes in a sodium acetate buffer (50 mM, pH 5.0). The amount of calcein released from the liposomes was monitored by the fluorescence intensity.

### 2.7. CD33 Expression and Cellular Uptake of Fluorescence-Labeled aCD33LN/GTI-2040

Kasumi-1 (high CD33 expression)[18] and K562 (low CD33 expression)[21] cells were used in this study. First, CD33 expression was confirmed using FITC-labeled aCD33. FITC labeled aCD33 was prepared as follows. FITC was dissolved in DMSO at a concentration of 10

mg/mL. Five-molar excess of FITC was added to aCD33 solution (2 mg/mL) and incubated for 1 h at room temperature protected from light. Then, 100× glycine was added to stop the reaction. Excess glycine and hydrolyzed FITC were removed by purification on a PD-10 gel filtration column. The product aCD33-FITC was stored at 4 °C.

For cellular binding assay, $4 \times 10^5$ Kasumi-1 and K562 cells were incubated with 200 μg/mL aCD33-FITC in culture media containing 1% BSA for 2 h at 37 °C. Then, the cells were washed three times with cold PBS and then resuspended in 100 μL of PBS and examined by fluorescence microscope and flow cytometry.

Cellular uptake of targeted LNs in Kasumi-1 and K562 cells was investigated as follows. Briefly, $5 \times 10^5$ cells were incubated with 1 μM Cy5-labled GTI-2040 in aCD33LNs for 4 h at 37 °C. The cells were washed twice with cold PBS and then incubated with 5 μg/mL of Hoechst 33342 for 8 min at room temperature. Finally, the cells were washed twice with cold PBS and fixed with 4% *para*-formaldehyde and then were examined by fluorescence microscope.

### 2.8. Inhibition of R2 Gene Expression in Kasumi-1 Cells

Kasumi-1 cells were seeded in a 6-well culture plate at a density of $5 \times 10^5$ cells/mL and cultured for 18 h. Then, the cells were treated with free GTI-2040, scrambled control sGTI-2040 with targeted LNs (aCD33LN/sGTI-2040), LN/GTI-2040, or aCD33LN/GTI-2040 for 4 h. Fresh media were then added. After incubation for an additional 48 h, the cells were harvested to determine the expression of R2 mRNA by quantitative real-time reverse transcriptase polymerase chain reaction (qRT-PCR) and by Western blot assay.

RNA samples were extracted from the treated cells by the TRIzol reagent, and then the SuperScript III First-Strand Synthesis System (Life Technologies, Carlsbad, CA, USA) was used to synthesize the cDNA. The resulting cDNA was amplified by qPCR using Taqman Universal Master Mix. Housekeeping gene 18S rRNA was used as endogenous control to normalize R2 mRNA expression.

R2 protein was extracted from the cell lysate and evaluated by Western blot. GAPDH was selected as a protein control to normalize the R2 protein level.

### 2.9. MTS Cell Viability Assay

Cell viability in response to GTI-2040 and Ara-C was studied by the MTS assay (Promega, Madison, WI, USA). Briefly, Kasumi-1 and K562 cells were seeded at a density of $5 \times 10^3$ cells/well in a 96-well plate and treated with PBS, GTI-2040, LN/GTI-2040, or aCD33LN/GTI-2040. After 4 h incubation at 37 °C, serial diluted Ara-C (0.0001–100 μM) solutions were added and the cells were incubated for an additional 48 h. MTS solution was then added to each well as described previously.[7] Cell viability was determined by measuring the absorbance of each well at 490 nm on an automated plate reader (Molecular Devices, Sunnyvale, CA, USA). $IC_{50}$ values were then calculated based on the measured absorbances.

### 2.10. Tumor Growth Inhibition and down Regulation of Intratumoral R2 Expression by aCD33LN/GTI-2040 in a Kasumi-1 Xenograft Model

Eight-week old female nonobese diabetic severe combined immunodeficient (NOD-SCID) mice were obtained from Jackson Lab (Bar Harbor, ME, USA). Mice were subcutaneously injected with Kasumi-1 cells (100 μL) at a density of $5 \times 10^7$ cells/mL. When the tumor volume reached approximately 100 $mm^3$, the inoculated mice were randomly divided into four groups (four mice per group). PBS, GTI-2040, LN/GTI-2040, or aCD33LN/GTI-2040 were administered by tail vein injection every 3 days for four times. Tumor size was measured using a Vernier caliper and its volume was calculated by the formula: tumor volume ($mm^3$) = 0.5 × length (mm) × width (mm) × height (mm). At 24 h following the final injection, mice were scarified and tumors were collected for analysis of R2 gene expression by qRT-PCR. Data were analyzed by *t* test. Differences between group means were considered statistically significant at $p < 0.05$.

### 2.11. Antitumor Activity of aCD33LN/GTI-2040 in Combination with Ara-C in a Kasumi-1 Xenograft Model

Eight-week old female NOD-SCID mice were subcutaneously injected with Kasumi-1 cells (100 μL) at a density of $5 \times 10^7$ cells/mL. When the tumor volume reached approximately 100 $mm^3$, the inoculated mice were randomly divided into five groups (six mice per group). PBS, GTI-2040, LN/GTI-2040, or aCD33LN/GTI-2040 were administered by tail vein injection once every 3 days. Following the second treatment, Ara-C (50 mg/kg) was coadministrated to mice by tail vein injection. Four injections were performed in total. Tumor size was measured using a Vernier caliper and volume was calculated by the formula: tumor volume ($mm^3$) = 0.5 × length (mm) × width (mm) × height (mm). The mice with tumor sizes over 1200 $mm^3$ were sacrificed, according to the established early removal criteria. Animal survival data in different groups were analyzed by the logrank test. $p < 0.05$ was considered a cutoff for a significant difference.

## 3. RESULTS AND DISCUSSION

### 3.1. Characterization of DOC-PEI and LN/GTI-2040

The reaction scheme for synthesis of DOC-PEI is shown in Figure 1. The structure of this conjugate was confirmed by $^1H$ NMR and FT-IR spectroscopy. The carbonyl group peak at 1650 $cm^{-1}$ in the FT-IR spectrum (Figure 2A) corresponds to the amide bond of DOC-PEI. From the $^1H$ NMR analysis (Figure 2B), the molar ratio of DOC to PEI-2K in the final product was determined to be approximately 3:1.

The particle size and zeta potential of LN/GTI-2040 was 85 ± 15 nm and 7.6 ± 0.3 mV, respectively. In contrast, the particle size and zeta potential of aCD33LN/GTI-2040 were 93 ± 18 nm and 4.3 ± 0.2 mV, respectively. Agarose gel retardation study was carried out and showed a complete retardation of GTI-2040 in the LNs and aCD33LNs (data not shown). Taken together, these data suggest that the cationic LNs and aCD33LNs can efficiently interact with the anionic GTI-2040 and form nanoparticles.

### 3.2. Effect of DOC-PEI as an LN Component on Transfection Efficiency

The effect of the DOC-PEI component on transfection efficiency was investigated in Kaumi-1 cells. As shown in Figure 3, significant greater downregulation of R2 protein was observed in the LN treatment groups compared to other groups. LNs containing DOC-PEI were more efficacious than LNs containing PEI-2K. This shows that DOC-PEI is a useful helper component in the LN formulation and is more effective than the unmodified PEI-2K. This may be due to a membrane lytic activity of DOC-PEI. To evaluate this hypothesis, calcein liposomes were prepared as a model for cellular membrane. Calcein is a membrane impermeable fluorescent dye and was encapsulated at a self-quenching concentration. Release of calcein is mediated by membrane lysis and can be detected by an increase in fluorescence signal due to dequenching. DOC-PEI and PEI-2K were evaluated for their ability to induce calcein release. The results are shown in Figure 4. The fluorescent intensity of the DOC-PEI group was significantly higher than that of the PEI-2K treatment group, indicating that DOC-PEI can better facilitate membrane disruption than PEI-2K. DOC-PEI is an amphiphilic agent previously shown to promote the delivery of siRNA.[22] The PEI moiety provides a polycation that electrostatically binds negatively charged ASO, undergoes pH-dependent protonation, and produces a proton sponge effect. Meanwhile, the DOC moiety facilitates ASO condensation and adds to the membrane lytic activity of the nanoparticles. These activities are shown by the hemolytic effect of DOC-PEI at acidic pH and its ability to induce content release from calcein-containing liposomes (Figure 4).

### 3.3. CD33 Expression and aCD33LN Uptake

Expression of CD33 by Kasumi-1 and K562 cells was evaluated by fluorescence microscopy and flow cytometry. As shown in Figure 5A,B, significant binding of aCD33-FITC was observed in Kasumi-1 cells, but not in K562 cells, indicating high level CD33 expression in Kasumi-1 cells. When these cells were treated with aCD33LNs loaded with Cy5-labeled GTI-2040, significantly higher uptake was observed in Kasumi-1 cells compared to K562 cells, which have low CD33 expression (Figure 5C). These results indicated aCD33LN/GTI-2040 selectively targeted CD33 positive Kasumi-1 cells.

### 3.4. Inhibition of R2 Gene Expression in Kasumi-1 Cells

Inhibition of R2 gene expression by GTI-2040 loaded LNs was investigated at a GTI-2040 concentration of 1 $\mu$M. As shown in Figure 6A, GTI-2040 alone was unable to reduce R2 mRNA expression. Significant down regulation of R2 was observed when the cells were treated with LN/GTI-204. aCD33LN/GTI-2040 showed the highest level of downregulation. R2 expression was reduced to 16 ± 9% relative to the untreated cells. The nontargeted LNs achieved reduced downregulation to 24 ± 7%. However, no significant difference was observed between groups treated with LN/GTI-2040 and aCD33LN/GTI-2040. This result can in part be explained by the reduction of zeta potential of aCD33LN/GTI-2040 compared to LN/GTI-2040, which was taken up by cells due to electrostatic interaction. The aCD33LNs with the control sGTI-2040, which was not matched to R2 mRNA but maintained the same base composition, did not induce downregulation of R2. Western blot results assessing R2 protein levels were consistent with those of qRT-PCR, as shown in

Figure 6B. These results indicate that the LNs, especially aCD33LNs were highly effective as delivery vehicles for ASOs such as GTI-2040.

### 3.5. $IC_{50}$ Modulation by aCD33LN/GTI-2040 in Kasumi-1 Cells

Prior studies have indicated a therapeutic benefit of combining GTI-2040 with Ara-C in the treatment of AML.[23] In this study, aCD33LN/GTI-2040 and Ara-C were evaluated as a combination in Kasumi-1 and K562 cells. $IC_{50}$ values were determined by MTS assay. The results are shown in Table 1. The $IC_{50}$ of Ara-C combined with LN/GTI-2040 was decreased nearly 4-fold relative to Ara-C combined with free GTI-2040 in both Kasumi-1 and K562 cells. Remarkably, aCD33LN/GTI-2040 induced a 2.8-fold greater Kasumi-1 cell chemosensitivity to Ara-C compared to LN/GTI-2040, which indicated that the CD33 targeting greatly improved the delivery of GTI-2040 to cells, thus potentiating its efficacy. In contrast, aCD33LN/GTI-2040 induced a 1.5-fold decreased K562 cell chemosensitivity to Ara-C compared to LN/GTI-2040, possibly resulting from a reduction of zeta potential of aCD33LN/GTI-2040 compared to LN/GTI-2040. Taken together, these results suggest that aCD33LN/GTI-2040 selectively targeted CD33 positive Kasumi-1 cells.

### 3.6. Tumor Growth Inhibition and Downregulations of Intratumoral R2 Expression in a Kasumi-1 Xenograft Model

Antitumor activity of aCD33LN/GTI-2040 was investigated in Kasumi-1 tumor-bearing mice. The tumor volume was significantly inhibited by free GTI-2040, LN/GTI-2040, and aCD33LN/GTI-2040 at 12 days after treatment compared to the PBS control (Figure 7A). Among the treatment groups, aCD33LN/GTI-2040 treated mice showed the most prominent tumor inhibition. All animals tolerated the treatments well with no observable signs of toxicity or change in body weight over the course of the study (data not shown). Therefore, DOC-PEI incorporated into LNs did not induce significant toxicity to mice. This is because the amount of DOC-PEI required for ASO delivery is low and DOC-PEI is complexed to ASO, which reduces its lytic activity prior to endocytosis. Consistent with this tumor growth inhibition, aCD33LN/GTI-2040 significantly downregulated R2 expression compared to LN/GTI-2040 or PBS control ($p < 0.05$). LN/GTI-2040 showed 15.5% decreased R2 expression compared to PBS control. However, no R2 mRNA downregulation was found in the treatment group of free GTI-2040 (Figure 7B). LN/GTI-2040, with its high zeta potential, did not operate *in vivo* due to the presence of high concentration of negatively charged plasma proteins. This gave the edge to aCD33LN/GTI-2040, which could mediate CD33-depenent uptake by the CD33+ target cells. Taken together, these data suggested that the antitumor activity of aCD33LN/GTI-2040 might be due to the downregulation of R2 protein.

### 3.7. Therapeutic Activity of aCD33LN/GTI-2040 in Combination with Ara-C in Kasumi-1 Xenograft Tumor-Bearing Mice

Antitumor activity of aCD33LN/GTI-2040 in combination with Ara-C was investigated in Kasumi-1 tumor-bearing mice. As shown in Figure 8A, tumor growth inhibition was most prominent in the group treated with aCD33LN/GTI-2040 combined with Ara-C. The survival rates of tumor-bearing mice in different treatment groups are shown in Figure 8B, and statistical analysis of the data are shown in Table 2. As expected, Ara-C, free GTI-2040

with Ara-C, LN/GTI-2040 with Ara-C, and aCD33LN/GTI-2040 with Ara-C all increased the survival rate of tumor-bearing mice compared to PBS group ($p < 0.01$). However, no significant difference was detected among the Ara-C only, free GTI-2040 with Ara-C, and LN/GTI-2040 with Ara-C groups. aCD33LN/GTI-2040 combined with Ara-C demonstrated the greatest antitumor activity in our study and displayed a significant difference from the nontargeted LN/GTI-2040 group ($p < 0.05$). This result correlated with the intratumoral R2 mRNA downregulation by aCD33LN/GTI-2040. Therefore, the potent antitumor activity of aCD33LN/GTI-2040 in combination with Ara-C might be due in part to the greater efficiency in delivery of GTI-2040 by aCD33LNs and the subsequent downregulation of R2 protein, which in turn reduced the endogenous level of dCTP and improved the antitumor activity of Ara-C.

## 4. CONCLUSION

In this study, a novel helper component for LNs, DOC-PEI, was synthesized and incorporated into the LN formulation. The addition of DOC-PEI significantly improved the transfection efficiency of the LNs due to its ability to facilitate endosomal membrane disruption. When cells were treated with aCD33LN/GTI-2040, significant uptake was observed in CD33 positive Kasumi-1 cells. LN/GTI-2040 and aCD33LN/GTI-2040 were then shown to efficiently induce downregulation of R2 protein expression in Kasumi-1 cells, both showing greater R2 downregulation than free GTI-2040. In Kasumi-1 xenograft model, aCD33LN/GTI-2040 showed significant R2 downregulation compared to LN/GTI-2040. Moreover, significant greater inhibition of tumor growth and prolonged survival time were observed when aCD33LN/GTI-2040 was coadministered with Ara-C, suggesting this therapeutic combination as a promising potential treatment for acute myelogenous leukemia (AML). Taken together, these data showed that aCD33LNs are potent targeted delivery vehicles for ASO to AML cells and warrant further evaluation.

## ACKNOWLEDGMENTS

This work was supported by NIH Grant R01CA135243.

## REFERENCES

(1). Dean NM, Bennett CF. Antisense oligonucleotide-based therapeutics for cancer. Oncogene. 2003; 22(56):9087–9096. [PubMed: 14663487]

(2). Jaschinski F, Rothhammer T, Jachimczak P, Seitz C, Schneider A, Schlingensiepen KH. The antisense oligonucleotide trabedersen (AP 12009) for the targeted inhibition of TGF-$\beta$2. Curr. Pharm. Biotechnol. 2011; 12(12):2203–2213. [PubMed: 21619536]

(3). Martínez T, Wright N, López-Fraga M, Jiménez AI, Pañeda C. Silencing human genetic diseases with oligonucleotide-based therapies. Hum. Genet. 2013; 132(5):481–493. [PubMed: 23494242]

(4). Hair P, Cameron F, McKeage K. Mipomersen sodium: first global approval. Drugs. 2013; 73(5): 487–493. [PubMed: 23564617]

(5). Rait AS, Pirollo KF, Xiang L, Ulick D, Chang EH. Tumor-targeting, systemically delivered antisense HER-2 chemosensitizes human breast cancer xenografts irrespective of HER-2 levels. Mol. Med. 2002; 8:475–486. [PubMed: 12435858]

(6). Zhao XB, Lee RJ. Tumor-selective targeted delivery of genes and antisense oligodeoxyribonucleotides via the folate receptor. Adv. Drug Delivery Rev. 2004; 56:1193–1204.

(7). Jin Y, Liu S, Yu B, Golan S, Koh CG, Yang J, Huynh L, Yang X, Pang J, Muthusamy N, Chan KK, Byrd JC, Talmon Y, Lee LJ, Lee RJ, Marcucci G. Targeted delivery of antisense oligodeoxynucleotide by transferrin conjugated pH-sensitive lipopolyplex nanoparticles: a novel oligonucleotide-based therapeutic strategy in acute myeloid leukemia. Mol. Pharmaceutics. 2010; 7(1):196–206.

(8). Yang X, Koh CG, Liu S, Pan X, Santhanam R, Yu B, Peng Y, Pang J, Golan S, Talmon Y, Jin Y, Muthusamy N, Byrd JC, Chan KK, Lee LJ, Marcucci G, Lee RJ. Transferrin receptor-targeted lipid nanoparticles for delivery of an antisense oligodeoxyribonucleotide against Bcl-2. Mol. Pharmaceutics. 2009; 6(1):221–230.

(9). Prakash TP, Lima WF, Murray HM, Elbashir S, Cantley W, Foster D, Jayaraman M, Chappell AE, Manoharan M, Swayze EE, Crooke ST. Lipid nanoparticles improve activity of single-stranded siRNA and gapmer antisense oligodeoxyribonucleotide in animals. ACS Chem. Biol. 2013; 8:1402–1406. [PubMed: 23614580]

(10). Jemal A, Siegel R, Ward E, Murray T, Xu J, Smigal C, Thun MJ. Cancer statistics, 2006. CA Cancer J. Clin. 2006; 56:106–130. [PubMed: 16514137]

(11). Lowenberg B, Downing JR, Burnett A. Acute myeloid leukemia. N. Engl. J. Med. 1999; 41(14): 1051–1062. [PubMed: 10502596]

(12). Lee Y, Vassilakos A, Feng N, Lam V, Xie H, Wang M, Jin H, Xiong K, Liu C, Wright J, Young A. GTI-2040, an antisense agent targeting the small subunit component (R2) of human ribonucleotide reductase, shows potent antitumor activity against a variety of tumors. Cancer Res. 2003; 63:2802–2811. [PubMed: 12782585]

(13). Klisovic RB, Blum W, Wei X, Liu S, Liu Z, Xie Z, Vukosavljevic T, Kefauver C, Huynh L, Pang J, Zwiebel JA, Devine S, Byrd JC, Grever MR, Chan K, Marcucci G. Phase I study of GTI-2040, an antisense to ribonucleotide reductase, in combination with high-dose cytarabine in patients with acute myeloid leukemia. Clin. Cancer Res. 2008; 14(12):3889–3895. [PubMed: 18559610]

(14). Simard P, Leroux JC. pH-sensitive immunoliposomes specific to the CD33 cell Surface antigen of leukemic cells. Int. J. Pharm. 2009; 381(2):86–96. [PubMed: 19446624]

(15). Simard P, Leroux JC. In vivo evaluation of pH-sensitive polymer-based immunoliposomes targeting the CD33 antigen. Mol. Pharmaceutics. 2010; 7(4):1098–1107.

(16). Kung Sutherland MS, Walter RB, Jeffrey SC, Burke PJ, Yu C, Kostner H, Stone I, Ryan MC, Sussman D, Lyon RP, Zeng W, Harrington KH, Klussman K, Westendorf L, Meyer D, Bernstein ID, Senter PD, Benjamin DR, Drachman JG, McEarchern JA. SGN-CD33A: a novel CD33-targeting antibody-drug conjugate using a pyrrolobenzodiazepine dimer is active in models of drug-resistant AML. Blood. 2013; 122(8):1455–1463. [PubMed: 23770776]

(17). Walter RB, Gooley TA, van der Velden VH, Loken MR, van Dongen JJ, Flowers DA, Bernstein ID, Appelbaum FR. CD33 expression and p-glycoprotein-mediated drug efflux inversely correlate and predict clinical outcome in patients with acute myeloid leukemia treated with gemtuzumab ozogamicin monotherapy. Blood. 2007; 109(10):4168–4170. [PubMed: 17227830]

(18). Rothdiener M, Müller D, Castro PG, Scholz A, Schwemmlein M, Fey G, Heidenreich O, Kontermann RE. Targeted delivery of siRNA to CD33-positive tumor cells with liposomal carrier systems. J. Controlled Release. 2010; 144(2):251–258.

(19). Yang X, Peng Y, Yu B, Yu J, Zhou C, Mao Y, Lee LJ, Lee RJ. A covalently stabilized lipid-polycation-DNA (sLPD) vector for antisense oligonucleotide delivery. Mol. Pharmaceutics. 2011; 8(3):709–715.

(20). Xu S, Liu Y, Tai HC, Zhu J, Ding H, Lee RJ. Synthesis of Transferrin (Tf) conjugated liposomes via Staudinger ligation. Int. J. Pharm. 2011; 404(1–2):205–210. [PubMed: 21056642]

(21). Chen P, Wang J, Hope K, Jin L, Dick J, Cameron R, Brandwein J, Minden M, Reilly RM. Nuclear localizing sequences promote nuclear translocation and enhance the radiotoxicity of the anti-CD33 monoclonal antibody HuM195 labeled with 111In in human myeloid leukemia cells. J. Nucl. Med. 2006; 47(5):827–836. [PubMed: 16644753]

(22). Kim D, Lee D, Jang YL, Chae SY, Choi D, Jeong JH, Kim SH. Facial amphipathic deoxycholic acid-modified polyethyleneimine for efficient MMP-2 siRNA delivery in vascular smooth muscle cells. Eur. J. Pharm. Biopharm. 2012; 81(1):14–23. [PubMed: 22311297]

(23). Chen P, Aimiuwu J, Xie Z, Wei X, Liu S, Klisovic R, Marcucci G, Chan KK. Biochemical modulation of aracytidine (Ara-C) effects by GTI-2040, a ribonucleotide reductase inhibitor, in K562 human leukemia cells. AAPS J. 2011; 13(1):131–140. [PubMed: 21191677]

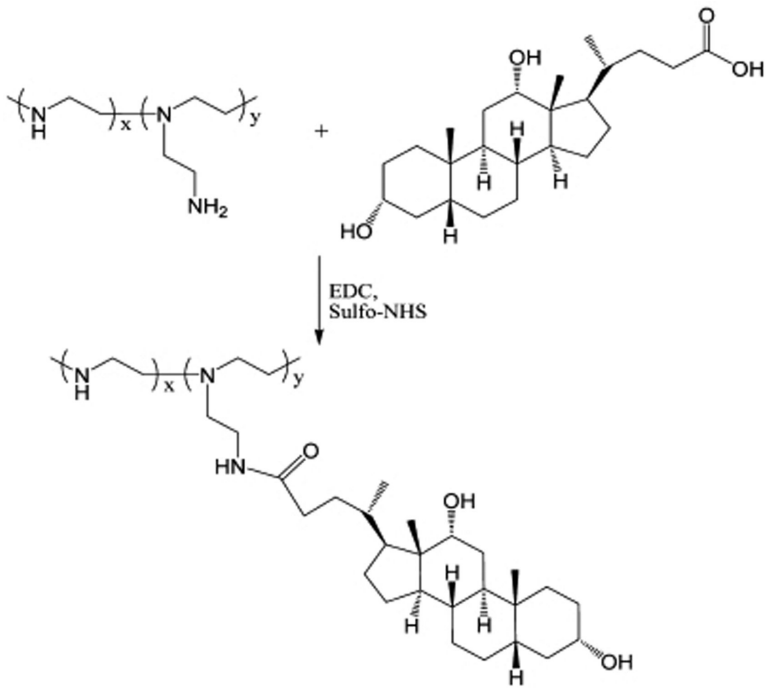


**Figure 1.**
Reaction scheme for the synthesis of DOC-PEI.

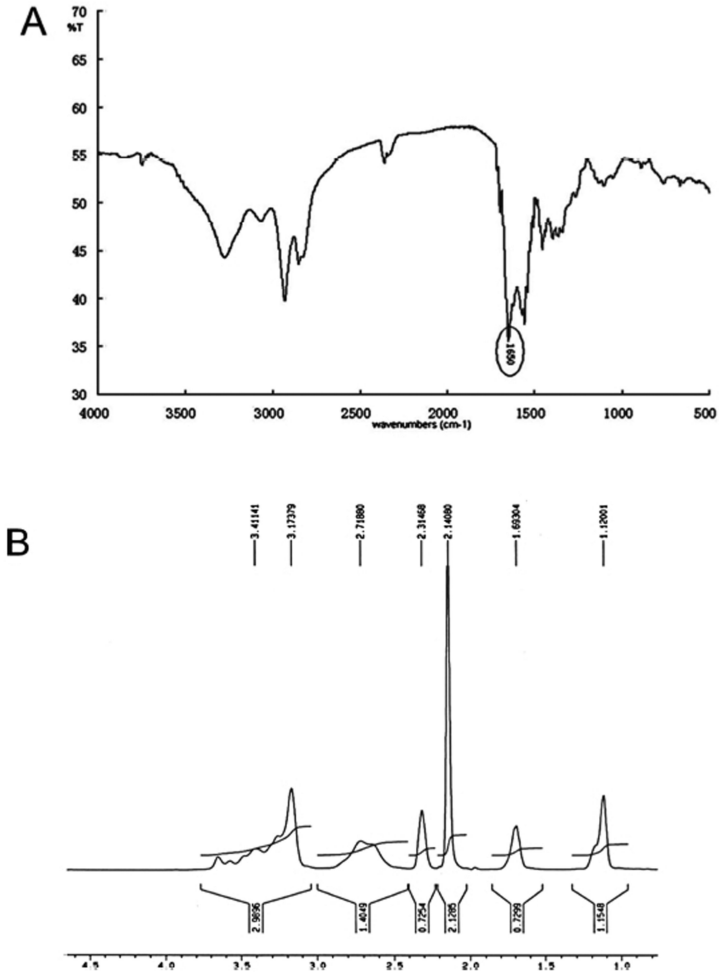


**Figure 2.**
Characterization of DOC-PEI: (A) FT-IR and (B) $^{1}$H NMR spectra.

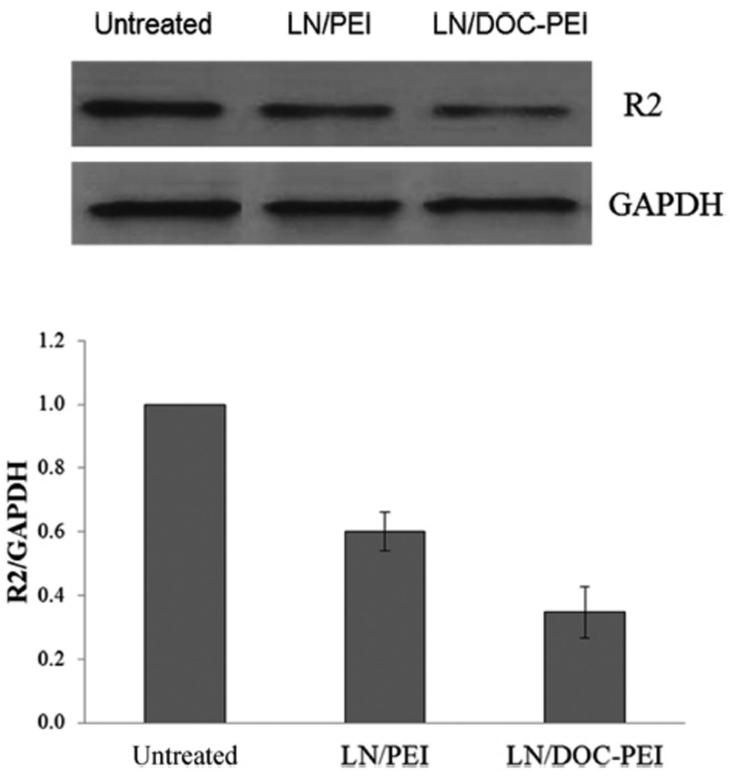


**Figure 3.**

Effect of DOC-PEI as a helper component in LNs on transfection efficiency. R2 protein expression in Kasumi-1 cells treated by PBS, LN/GTI-2040 with PEI, or DOC-PEI ($n = 3$). GTI-2040 was administered at 1 $\mu$M. Upper panel shows the representative Western blot image and lower panel shows the average densitometry data.

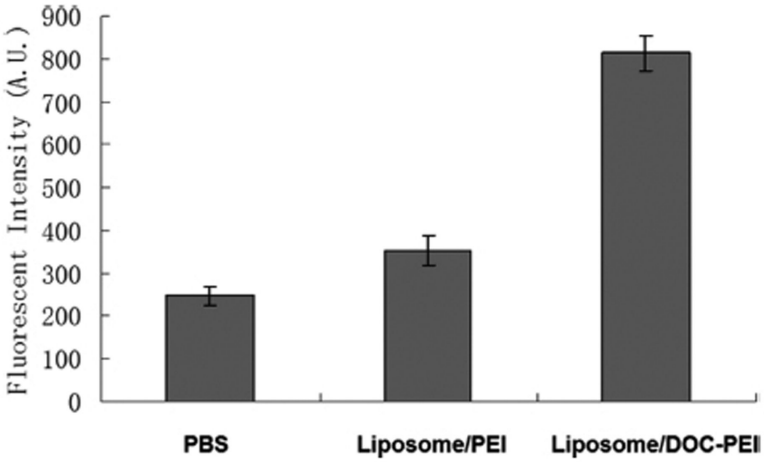


**Figure 4.**

Calcein release from liposomes with PEI or DOC-PEI. Calcein liposomes were incubated with PBS, liposome/PEI, or liposome/DOC-PEI ($n = 3$).

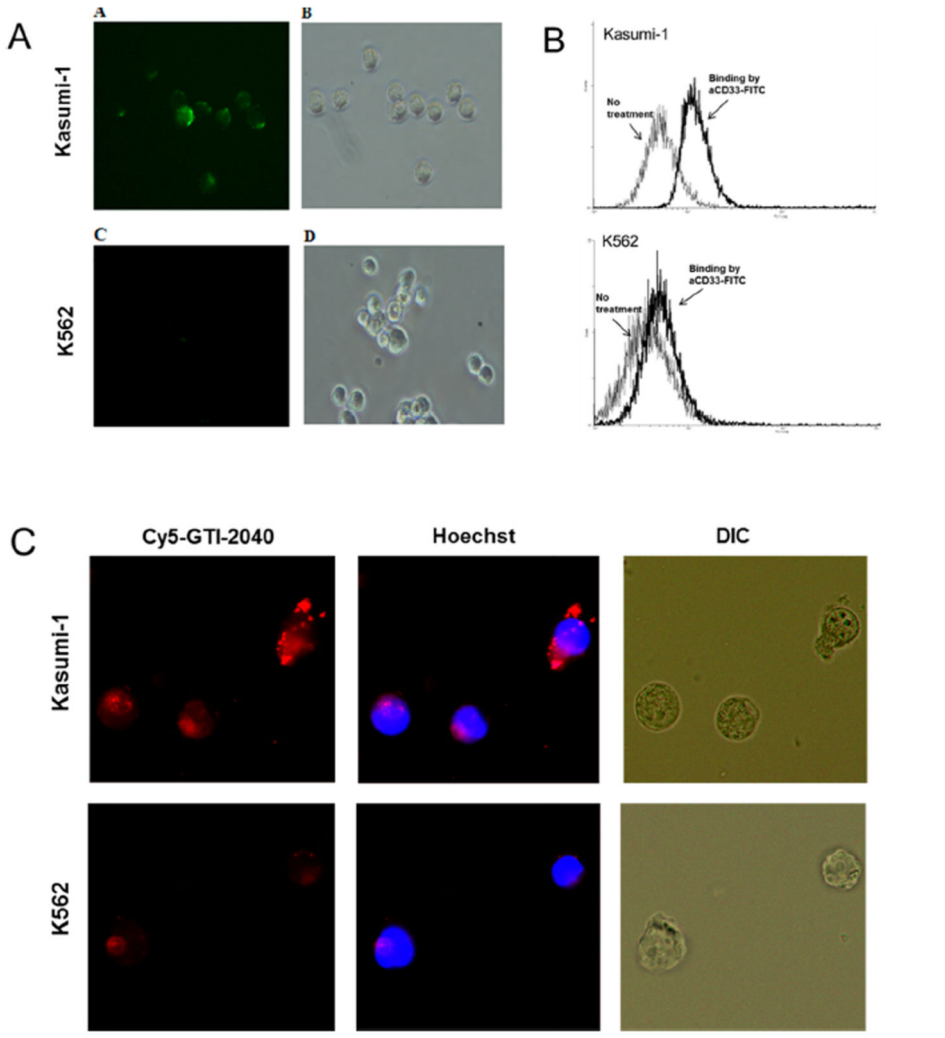


**Figure 5.**

Binding of aCD33-FITC and uptake of aCD33LN loaded with Cy5-GTI-2040 in Kasumi-1 and K562 cells. Binding of aCD33-FITC to cells were visualized by fluorescence microscope (A) and flow cytometry (B). Uptake of aCD33LN (C) was observed by fluorescence microscope. Cells were treated with Cy5-GTI-2040 (red) in aCD33LNs, and DNA was stained with Hoechst 33342 (blue).

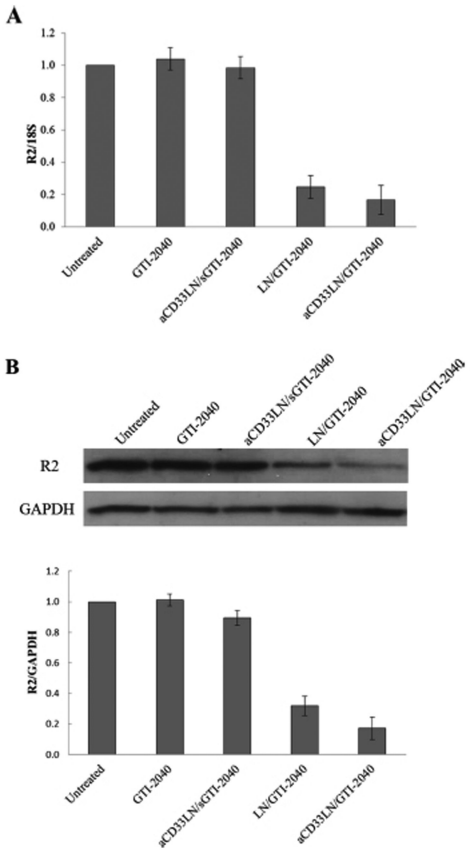


**Figure 6.**

R2 gene expression in Kasumi-1 cells. Cells were treated with 1 $\mu$M GTI-2040 in various formulations. (A) R2 mRNA expressions were analyzed by qRT-PCR ($n$ = 3). (B) R2 protein expressions were analyzed by Western blot ($n$ = 3). Upper panel shows the representative Western blot image and lower panel shows the average densitometry data.

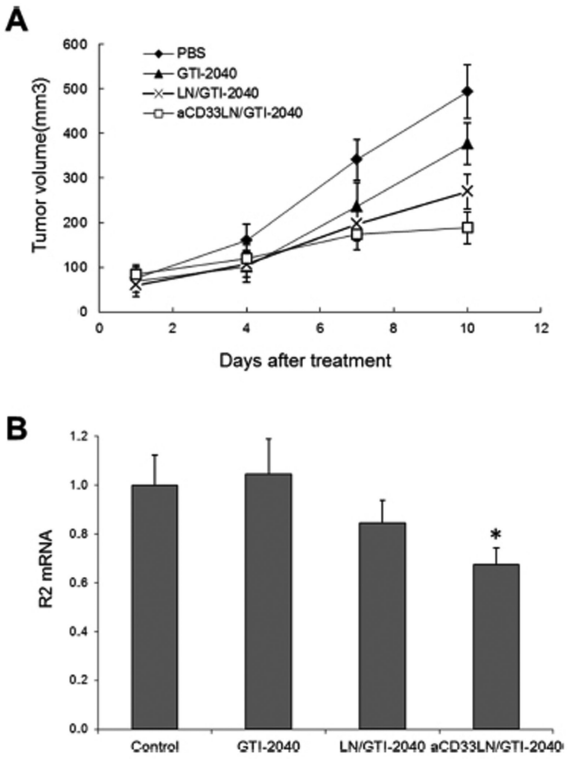


**Figure 7.**

Tumor growth inhibition and downregulation of intratumoral R2 expression in Kasumi-1 xenograft tumor-bearing mice. Tumor-bearing mice ($n = 4$) were treated with various formulations of GTI-2040 (3 mg/kg), as described in Materials and Methods. (A) Inhibition of tumor growth. (B) Intratumoral R2 mRNA expression.

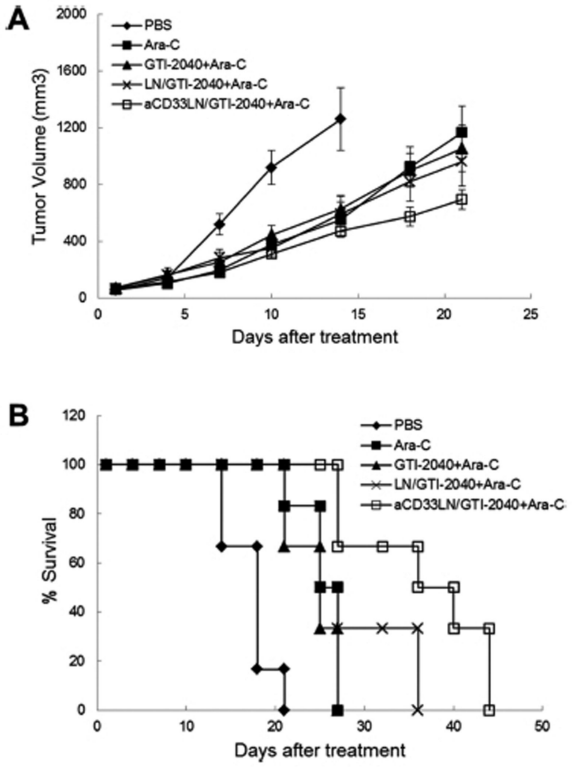


**Figure 8.**

Therapeutic activity of aCD33LN/GTI-2040 in combination with Ara-C in Kasumi-1 xenograft tumor-bearing mice. Tumor-bearing mice ($n = 6$) were treated with various formulations of GTI-2040 (3 mg/kg) and Ara-C (50 mg/kg), as described in Materials and Methods. (A) Inhibition of tumor growth. (B) Survival of the tumor-bearing mice.

**Table 1**

$IC_{50}$ of Different Treatment Groups to Ara-C in Kasumi-1 and K562 Cells; the Results Represent the Mean ± SD of Three Experiments

| $IC_{50}$ ($\mu$M) | Ara-C | GT1-2040 | LN/GT1-2040 | aCD33LN/CT1-2040 |
|---|---|---|---|---|
| Kasumi-1 | 3.83 ± 0.32 | 3.10 ± 0.23 | 0.65 ± 0.16 | 0.24 ± 0.06 |
| K562 | 8.24 ± 0.42 | 6.25 ± 0.45 | 1.65 ± 0.31 | 2.53 ± 0.35 |

**Table 2**

Statistical Analysis of the Antitumor Activity of Various Treatments on Kasumi-1 Tumor-Bearing Mice

| groups | log-rank *p* value[a] |
|---|---|
| PBS | |
| Ara-C | 0.00146 |
| GT1-2040 + Ara-C | 0.00266 (0.515[b]) |
| LN/CT1-2040 + Ara-C | 0.00146 (0.417[b]) |
| aCD33LN/CTI-2040 + Ara-C | 0.000604 (0.00896,[b] 0.0403[c]) |

[a]The *p* values were calculated relative to PBS.

[b]The *p* values were calculated relative to Ara-C.

[c]The *p* values were calculated relative to LN/GTI-2040.